

COLD BASIN IN COASTAL RANGE, EASTERN TAIWAN: INFERRED FROM ARGON RETENTION IN ZEOLITE AND ALTERED GLASS DURING BURIAL HEATING

CHING-HUA LO, SU-CHIN CHANG, WEN-SHAN CHEN AND SHENG-RONG SONG

Department of Geosciences, National Taiwan University, Taipei, Taiwan

ABSTRACT

$^{40}\text{Ar}/^{39}\text{Ar}$ dating of altered glass and zeolite extracted from the volcanic basement of the West Taiyuan Basin, Coastal Range, was conducted to quantifying possible temperature conditions in the basin. Relatively young plateau dates of 3.4~3.8 Ma were obtained for altered glass and zeolite, which are much younger than that obtained for a fresh andesite from the same outcrop (5.8 ± 0.2 Ma) and the depositional age of the basal formation (~5.1 Ma). These young plateau dates may indicate the age of diagenetic alteration, if the temperature condition in the basin was low enough. A diffusion model suggests that an extremely low geothermal gradient was necessary to retain radiogenic argon in the present altered glass and zeolite. On the basis of argon loss calculations, the geothermal gradient of this orogenic basin in Coastal Range was likely $< \sim 10^\circ\text{C}/\text{km}$. This value is considerably lower than those found in other ordinary basins on the Earth's surface.

Key words: Coastal Range, eastern Taiwan, argon retention, cold basin

INTRODUCTION

Understanding the thermal evolution of sedimentary basins is fundamentally important to a variety of geological disciplines for the reasons related to economics and lithosphere tectonics. Since 1970, intense studies using various methods have been carried out for the purpose of revealing the thermal history of sedimentary basins (see McCulloh and Naeser, 1989, for a review). Basically, two fundamentally different approaches have evolved in the study of the thermal conditions and thermal evolution of sedimentary rocks. One approach is theoretical and inductive. It uses physical models that display causative mechanisms of basin inception, and takes into consideration acknowledged geological constraints derived from reflection seismic

data and geological analogies. The other approach is fundamentally empirical, descriptive and deductive. Observation data from wells and outcrops are gathered to permit interpretations about the thermal condition of the basin. In both approaches, observational and analytical data are essential for validation. As a consequence, a number of measures have been used with the aim of quantifying thermal conditions in sedimentary basins. These include techniques to measure the maturity of solid-phase organic materials (optical reflectance of vitrinite, thermal alteration indices of kerogen concentrates), molecular chemical indicators of organic matters (carbon preference index), equilibration of mineral assemblages or water-rock interactions (oxygen isotopic composition of neoformed diagenetic minerals and clay mineral assemblage) (c.f. Naeser and McCulloh, 1989). Unfortunately, the applications of these methods are limited to revealing the peak burial temperatures of the sediments during basin formation and cannot be directly applied to reveal the duration of burial heating. In order to further decipher the thermal history of a sedimentary basin, a number of techniques based on reaction kinetics have been used in an attempt to constrain the timing and thermal intensity of heating in sediments. These include the annealing process of fission tracks in detrital apatite (Gleadow *et al.*, 1983), Ar loss from detrital microcline (Harrison and B  , 1983; Girard and Onstott, 1991) and reaction of smectite-to-illite conversion (Huang *et al.*, 1993). The kinetics of these reaction processes are understood well enough that major features of burial thermal history can be deciphered from suitable sedimentary profiles.

On the basis of the kinetics of smectite-to-illite conversion model and the observation data of Dorsey *et al.*, (1988), Huang *et al.*, (1993) discovered an unusually low geothermal gradient ($\sim 1.64\text{--}2.62^\circ\text{C}/100\text{m}$) within the sedimentary basins in Coastal Range, East Taiwan. Indeed, the rapid uplifting of the young mountain belt in Taiwan potentially induced a rapid accumulation of young, cold sediments in the basins around the island. As a consequence, the low geothermal gradient may therefore be the result of the basin's high sedimentation rate. However, the high smectite/illite values in the sedimentary basins of the Coastal Range, East Taiwan, may also reflect a high relaxation rate of heat lasting from the volcanism and/or a low rate of smectite-to-illite conversion (Dorsey *et al.*, 1988). In order to further clarify the possible causes of the low geothermal gradient in the sedimentary basins of Coastal Range, the present study conducts a series of $^{40}\text{Ar}/^{39}\text{Ar}$ analyses on zeolite and altered glass from andesites which were deeply embedded in the bottom of the sedimentary basin in Coastal Range. Presumably, the measurement of argon loss from zeolite and altered glass, which is solely controlled by burial heating, should serve as an independent indicator of the thermal condition in the basin. Hopefully, an argon loss measurement will help quantify the thermal history of basins in Coastal Range, East Taiwan.

GEOLOGICAL BACKGROUND

The eastward subduction of the South China Sea Plate along the Manila Trench that commenced $\sim 17\text{--}35$ Ma ago (Suppe, 1988), created the Luzon magmatic arc which extends from Taiwan in the north, to Mindoro in the south. With the northwestward movement of the Philippine Sea Plate, the northern tip of the Arc was carried northwestward and began colliding with the Eurasian Continental Plate at Coastal Range of Taiwan about ~ 5 million years ago (Chi *et al.*, 1984, Suppe, 1984; Teng, 1990). Collision related mountain building, deformation, and flipping of subduction are all propagating southward along the Manila Trench at a rate of ~ 84 km/m.y. (Suppe, 1984). The history of the tectonic evolution of the arc-continent collision

around the South China Sea has been reviewed in detail by Suppe (1984) and Teng (1990). The collision has resulted not only in the rapid uplift of the accretionary prism forming the Taiwan Mountain Belt, but also the development of syn-orogenic basins around the mountain belt. In Coastal Range, many syn-orogenic basins were originally forearc or back-arc basins developed around the volcanoes in the Luzon Arc, and then became collisional basins during the progressive collision (Chen, 1988). Before the collision, the sediments were mainly clastic sediments, characterized by unmetamorphosed sandstone/mudstone derived from passive continental margin. In addition, there were some ophiolitic fragments and lithic clastics derived from the oceanic crust and arc volcanoes, forming olistrostromes and rhythmic turbidite sequences overlying the volcanic basement. With the propagation of the collision, the sedimentary composition in the basins became mainly conglomerates of slate, quartzite, schists with small amounts of metamorphosed ophiolitic fragments, which were presumably derived from the uplifted mountain belt (Chen, 1988; Dorsey *et al.*, 1988). Due to the rapid uplift of the Taiwan Mountain Belt during the collision, the high sedimentary rate induced a thick pile of sediments measuring 3~5 km in the basins in Coastal Range (Fig. 1). These sedimentary sequences non-conformably overlie the volcanic basement, which was formed during 16~5 Ma (Chen, 1988; Dorsey *et al.*, 1988; Lo *et al.*, 1994).

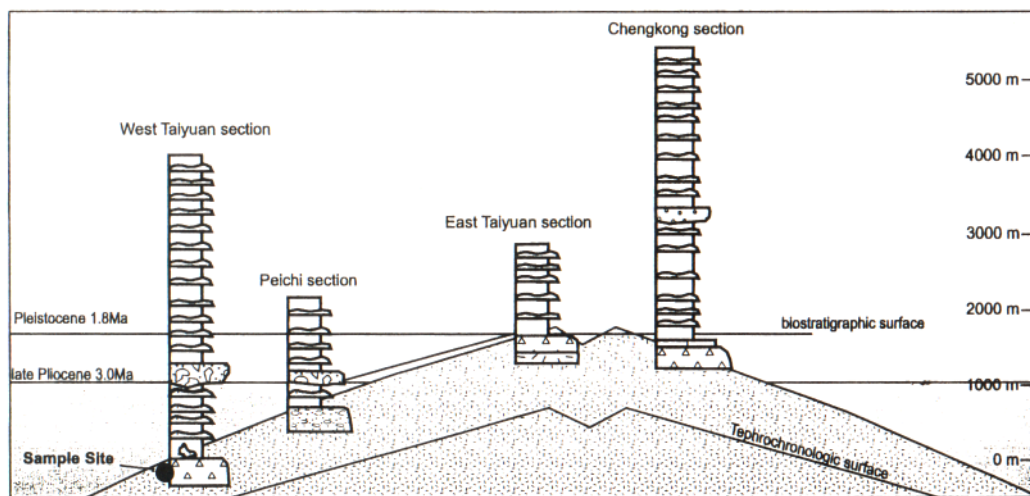


Figure 1. Stratigraphic column for the basins in the central part of the Coastal Range (after Chen, 1988), showing that the volcanic basement was once deeply buried by sediments during basin evolution. Note that the present samples were collected from an outcrop near Taiyuan Village, stratigraphically located at the top of the volcanic basement in Western Taiyuan Basin.

SAMPLES AND ANALYTICAL METHOD

Samples were collected from the volcanic basement of the West Taiyuan Basin in Coastal Range, cropping out near Taiyuan Village (Fig. 1). These include one fresh andesite sample

and two altered ones with zeolite crystals in cavities of altered andesites from the same outcrop. Similar to other basins in Coastal Range, the West Taiyuan Basin was once a forearc basin before the collision and became an orogenic basin afterwards. As a result, the basin is composed of a volcanic basement with a layer of overlying upper Miocene sandstone/mudstone rhythmites, which in turn is unconformably overlain by Pliocene-Pleistocene mudstone, turbidites and conglomerate derived from the metamorphic accretionary wedge of proto-Taiwan. The thickness of the sedimentary sequence has been estimated to be at least 4 km. This suggests that the volcanic basement was once deeply buried to a depth of about 4 km (Fig. 1) (Chen, 1988). Paleontologic data show that the basal formation of the West Taiyuan Basin was deposited about 5.1 Ma ago (Zone NN11) (Chi *et al.*, 1981).

One fresh andesite sample (DW3WR) and two altered andesite samples (DW1 and DW2) were collected from the top of the volcanic sequence near the bottom of the basin (Fig. 1). According to previous geochronological results, the volcanic eruption in Coastal Range started early Miocene (~17 Ma) and lasted until about 5 Ma (Lo *et al.*, 1994). The basal formation also started deposition at about 5 Ma (Chi *et al.*, 1981; Chen, 1988; Dorsey *et al.*, 1988; Teng, 1990). This infers that the age of the present samples should be older than ~5 Ma. This notation has been confirmed by field evidence that the volcanic complex is underlying late Miocene-early Pliocene sedimentary beds (Fig. 1) (Chen, 1988).

The present andesite samples display typical porphyritic texture, with phenocrysts of plagioclase, hornblende, pyroxene and iron oxides surrounded by a groundmass of fine-grained plagioclase and glass. In the altered samples (DW1 and DW2), hornblende and pyroxene phenocrysts have been replaced by an assemblage of chlorite + zoisite + sphene along the rim. Some plagioclase phenocrysts were saussuritized, but the groundmass plagioclase does not seem to have been affected. Rather, the groundmass glass has been palagonitized, causing it to exhibit a brown to brownish yellow color. However, without further detailed studies, the degree of palagonitization remains uncertain. In the following discussion, the term "altered glass" is adopted to describe the sample. In both altered samples, a significant amount of white-color zeolite crystals exist either as an interstitial phase between plagioclase phenocrysts or as radial aggregates in vesicles. X-ray diffraction data show that natrolite, tetranatrolite, laumontite and phillipsite are the major constitutive zeolite phases in these altered samples. Natrolite and laumontite appear to be the most abundant zeolite phases in DW2, while tetranatrolite is the most prominent phase in DW2, although both samples contain other zeolite phases in minor amount. According to Lan (1982), post-magmatic hydrothermal alteration under temperatures varying from 530°C to 200°C may have been responsible for the chloritization of amphibole and pyroxene in the volcanic rocks of East Coastal Range. Zeolites were formed at relatively low temperatures of about ~50-200°C either during the latest hydrothermal alteration or during diagenetic reactions in deep basin (Lan, 1982; Lo, 1987).

Whole-rock samples were crushed and lightly grounded to reduce loosely held atmospheric argon contamination. The 20-60 mesh fraction was selected for the $^{40}\text{Ar}/^{39}\text{Ar}$ dating analyses. Zeolite and altered glass were extracted from the samples by hand-picking under stereoscopic microscopy. Clean samples (~1-2 g) were then wrapped in aluminum foil packets, stacked with the irradiation LP-6 Biotite standard (Odins *et al.*, 1982) in an aluminum canister, and irradiated in the VT-C position of the THOR Reactor (National Tsing-Hua University, Hsin-Chu) for 10 hours. After irradiation, samples were loaded in degassed quartz boats, placed into a degassed fused quartz tube, baked at 200°C for 36 hours, and then degassed following a 20 minute/step schedule using a Lindberg resistance furnace. The temperature was controlled to within $\pm 1^\circ\text{C}$ by an Eurotherm controller. Two Pt-Rh thermocouples straddling the fused quartz tube monitored the temperature gradient across the sample region. The temperature gradient across

the tube was less than 2°C. Concordance between these two thermocouples suggests that the temperature estimates are not greatly in error. The purified gas was analyzed with a Varian-MAT GD150 mass spectrometer. Following procedures outlined in detail by Lo and Lee (1994), the concentrations of ^{36}Ar , ^{37}Ar , ^{38}Ar , ^{39}Ar and ^{40}Ar were corrected for system blanks, for radioactive decay of the nucleogenic isotopes, and for minor interference reactions involving Ca, K and Cl. The gradient of neutron flux across the irradiation canister was less than 0.5% as reflected in the J-value variation between the standards at the top and the bottom of the irradiation can. The $^{40}\text{Ar}/^{39}\text{Ar}$ analytical data were given in the Appendix, and were plotted as age spectrum and isotopic correlation diagrams in Figures 2 and 3, respectively.

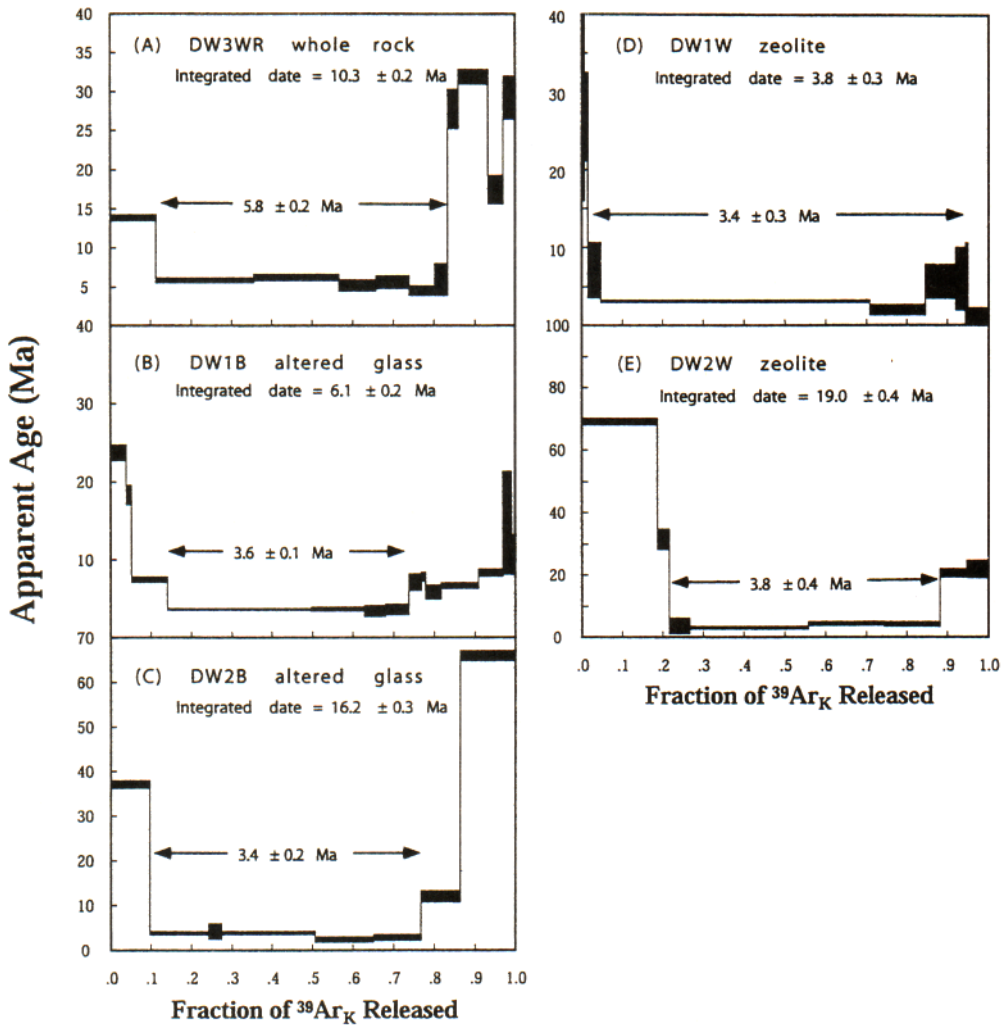


Figure 2. Apparent age spectra for all the samples analysed. The plateau date is given between the arrows and the arrows cover the gas fractions included into the calculation of the plateau date. The integrated date is given below the sample name. Boxes for each step extend vertically to $\pm 1\sigma$, and horizontally in proportion to the fraction of $^{39}\text{Ar}_K$ released in the step.

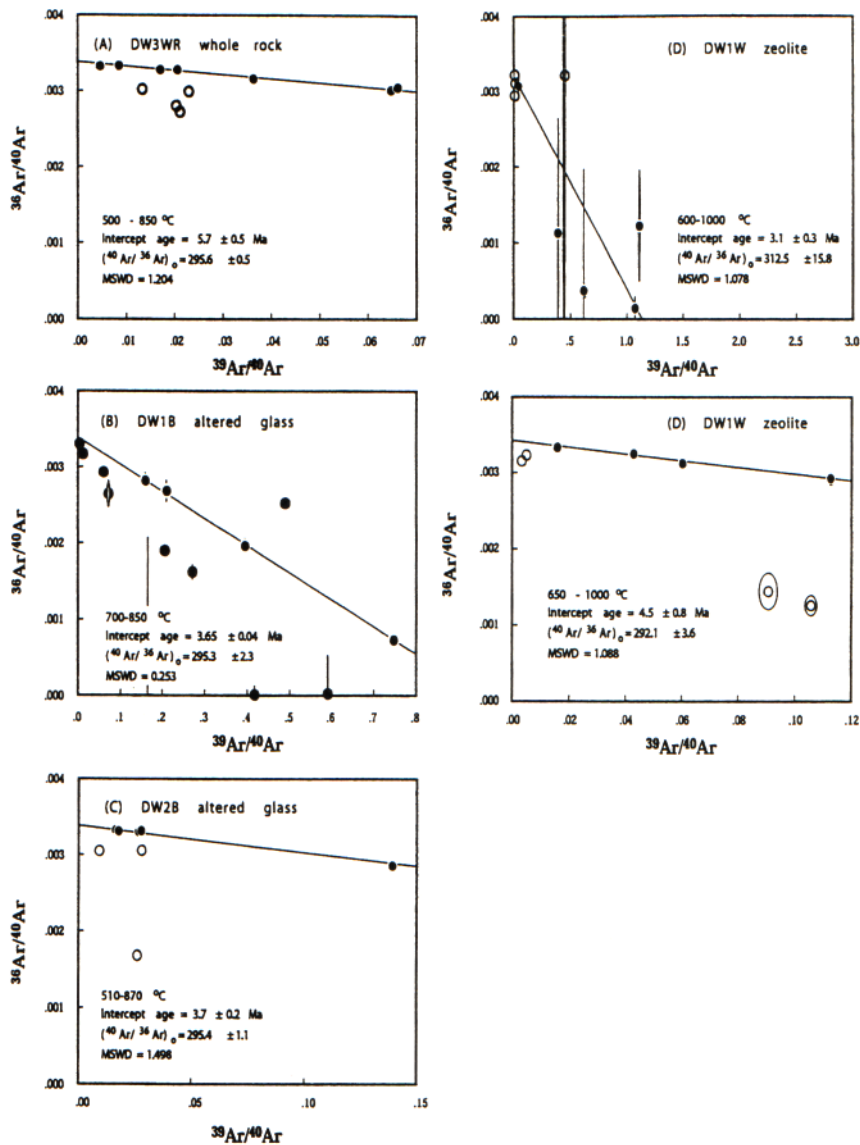


Figure 3. $^{36}\text{Ar}/^{40}\text{Ar}$ - $^{39}\text{Ar}/^{40}\text{Ar}$ isotope correlation diagrams for the samples analysed. The error ellipses are $\pm 1\sigma$. Solid circles indicate the isotopic compositions of plateau steps, which were utilized in the regression. Open circles are those for the discordant steps. Insert text shows the regression results.

Integrated dates were calculated from the sum total of the peak heights and their errors from the square root of the sum of squares of the peak height errors for all temperature steps. The plateau dates were calculated using the same approach, but utilizing only those temperature steps yielding dates on the plateau. As suggested by Lanphere and Dalrymple (1978), the

plateau was defined by: (1) at least four successive temperature steps with dates that fall within 2 σ of the average, provided that (2) the gas fraction for these plateau steps is more than 50% of the total ^{39}Ar released. Data for those temperature steps on the plateau were further plotted on the $^{36}\text{Ar}/^{40}\text{Ar}$ - $^{39}\text{Ar}/^{40}\text{Ar}$ isotopic correlation diagram which is widely utilized in the interpretation of $^{40}\text{Ar}/^{39}\text{Ar}$ experimental data (Roddick, 1978; McDougall and Harrison, 1999). The $^{40}\text{Ar}/^{39}\text{Ar}$ intercept dates and $^{40}\text{Ar}/^{36}\text{Ar}$ initial values were calculated from the intercepts of the regressed line. The cubic least-square fitting scheme outlined by York (1969) was employed in data regression.

ANALYTICAL RESULTS

As shown in Figure 2A, the fresh sample DW3WR displays a relatively flat age spectrum, with a reasonable plateau over the temperature range of 500–830°C, which comprises about 72% of the total $^{39}\text{Ar}_k$ released. Anomalous high dates appear in the lowest and highest temperature steps (Fig. 1A). According to Lo *et al.* (1994), these discordant dates may be the result of alteration effects or outgassing of phenocrysts, as inferred from the high $^{38}\text{Ar}_{cl}/^{39}\text{Ar}_k$ and $^{37}\text{Ar}_{ca}/^{39}\text{Ar}_k$ ratios in its isotopic composition (Appendix). The isotopic compositions for the plateau steps yield a plateau date of 5.8 ± 0.2 Ma. This is in perfect agreement with its corresponding intercept date of 5.7 ± 0.5 Ma, which was obtained from regression of isotopic data for the plateau steps in the isotopic correlation diagram (Figs. 2A and 3A). The $^{40}\text{Ar}/^{36}\text{Ar}$ intercept ($(^{40}\text{Ar}/^{36}\text{Ar})_o = 295.6 \pm 0.5$) and the mean sum of weighted deviation (MSWD) values (1.204) are all consistent with the atmospheric composition (295.5) and the cut-point value for meaningful regression which should be less than 10 (Fig. 3A). These suggest that the plateau date obtained from the step-heating experiment for the sample DW3WR should be geologically meaningful.

Two glass samples (DW1B and DW2B) of altered andesite yielded age spectrum profiles similar to the fresh sample (DW3WR), in which the apparent age decreases from 23–37 Ma at the lowest temperature, to ~3.4–3.6 Ma over the mid-temperature ranges, and then increases to 14–66 Ma at high temperatures (Figs. 2B and 2C). As reflected in the high $^{38}\text{Ar}_{cl}/^{39}\text{Ar}_k$ and $^{37}\text{Ar}_{ca}/^{39}\text{Ar}_k$ ratios (Appendix), the discordant dates in the low and high temperature steps are most likely due to outgassing of altered phenocrysts that were completely removed during sample separation. At mid-temperature steps, the isotopic compositions for both samples contained more than 59% of the total $^{39}\text{Ar}_k$ released, yielding similar plateau dates of 3.6 ± 0.1 Ma and 3.4 ± 0.2 Ma for the altered glass samples (DW1B and DW2B), respectively. Regression of isotopic data for these plateau steps, as shown in isotopic correlation diagrams, suggests almost identical intercept dates of 3.65 ± 0.04 Ma for DW1B and 3.7 ± 0.2 Ma for DW2B. These samples exhibit reasonable MSWD values (0.253 for DW1B and 1.498 for DW2B) and $^{40}\text{Ar}/^{36}\text{Ar}$ intercept values (295.3 ± 2.3 for DW1B and 295.4 ± 1.1 for DW2B), which is consistent with the atmospheric composition (295.5) (Figs. 3B and 3C). These findings suggest that the plateau dates should also be geologically meaningful, despite the fact that both plateau dates are much younger than that of the fresh sample (DW3WR, 5.8 ± 0.2 Ma) taken from the same outcrop.

Surprisingly, the two zeolite samples also yielded plateau dates (3.4 ± 0.3 Ma for DW1W and 3.8 ± 0.4 Ma for DW2W) indistinguishable from that of their respective altered glass samples (Figs. 3D and 3E). The age spectrum profiles are quite similar in shape and both display

anomalously old dates in the low and high-temperature steps, although, as discussed earlier, the modal abundances of different zeolite phases are different in these two samples. Isotopic correlation diagrams also show consistent intercept dates for these zeolites (3.1 ± 0.3 Ma for DW1W and 4.5 ± 0.8 Ma for DW2W) with their corresponding plateau dates and statistically reasonable $^{40}\text{Ar}/^{36}\text{Ar}$ intercept and MSWD values (312.5 ± 15.8 and 1.078 for DW1W and 292.1 ± 3.6 and 1.088 for DW2W). Similarly, these plateau dates should be geologically meaningful despite the fact that they are also much younger than the plateau date of the fresh sample.

DISCUSSIONS

Ages of Volcanic Eruption and Alteration Events

As discussed above, analyses of the isotopic compositions for the mid-temperature steps yielded plateau dates that are consistent with the criteria given by Lanphere and Dalrymple (1978) (Fig. 2). Isotope correlation diagrams suggest that the plateau dates are geologically meaningful, as reflected in reasonable $^{40}\text{Ar}/^{36}\text{Ar}$ intercept values and statistically meaningful MSWD values (Fig. 3). However, plateau dates for the altered glass and zeolite samples ($3.4 \sim 3.8$ Ma) are all much younger than that of the fresh whole rock sample (5.8 ± 0.2 Ma) taken from the same outcrop. The plateau date for the fresh sample DW3WR (5.8 ± 0.2 Ma) agrees well with the youngest $^{40}\text{Ar}/^{39}\text{Ar}$ dates (~ 5.6 Ma) for the volcanic rocks in Coastal Range, as reported by Lo *et al.*, (1994). In addition, they are also in agreement with many local stratigraphic relations and paleontologic data reported by Chi *et al.*, (1981), Huang *et al.*, (1988), Chen (1988) and Teng (1990), suggesting that the age of the arc-continent collision was around 5Ma. These findings also suggest that the volcanic basement in the West Taiyuan Basin may have formed approximately 5 million years ago. If this is the case, alteration reactions and diagenesis may have been responsible for lowering the $^{40}\text{Ar}/^{39}\text{Ar}$ ages of the altered samples used in the present study.

Lo *et al.*, (1994) suggested that the alteration reactions may result in either anomalously old dates due to zeolites (mainly phillipsite) absorbing excess argon, or anomalously young dates due to the loss of argon during the alteration reactions. In the case of the formation of phillipsites, the alteration reactions possibly induced the absorption of excess argon into the crystals. As a consequence anomalously old dates for the low-temperature steps resulted (Lo *et al.*, 1994). Alternatively, the alteration of mafic minerals or the palagonitization of glass, which commonly results in the formation of zoisite, chlorite, hydrous glass and oxides, often yields anomalously young dates due to recrystallization reactions. After careful examination of the outgassing behaviors of phases in andesite, Lo *et al.* (1994) concluded that during experimental heating, most of the argon in glass is released in the temperature range of $600\text{--}900^\circ\text{C}$, while chlorite releases argon at a temperature range below 650°C and most phenocrysts and zoisite at high temperatures of $>900^\circ\text{C}$. On the basis of this information, the anomalously old dates obtained for the low-temperature steps in zeolite and altered glass of the present study are most likely due to the outgassing of phillipsite, which is one of the alteration phases in the present samples, while the anomalously young dates obtained from the high temperature steps are most likely due to the presence of zoisite, phenocrysts and oxides. Argon released during the mid-temperature range is most likely due to the outgassing of glass (Lo *et al.*, 1994). Accordingly, the plateau dates of altered glass (3.6 ± 0.1 Ma for DW1B and 3.4 ± 0.2 Ma for DW2B) can be considered the age of alteration during subsequent diagenesis after it was buried. This notion is

supported by the consistency between the plateau dates of the altered glass samples and those for co-existing zeolites (mainly tetra-natrolite and natrolite) (3.4 ± 0.3 Ma for DW1W and 3.8 ± 0.4 Ma for DW2W). In addition, it is consistent with a number of observations: (1) these plateau dates are younger than the volcanic eruption age, as revealed by the plateau date of the fresh sample (5.8 ± 0.2 Ma, DW3WR)(Fig. 2A); (2) most zeolite phases, especially natrolite, tetranatrolite and laumontite, have long been considered to crystallize at low temperatures during burial diagenesis in basins in Coastal Range (Lo, 1987); and (3) as revealed by stratigraphic and paleontologic records, the plateau dates are also younger than the deposition age of basal formation in the West Taiyuan Basin (~ 5.1 Ma) (Chi *et al.*, 1981; Chen, 1988). However, their geological implications still need further exploration, because of the low argon retentivity of zeolite and glass, whose argon isotopic systematics are often subject to argon loss during burial heating (Barrer and Vaughan, 1971; Carroll and Stolper, 1991). If alteration reaction and crystallization of zeolites occurred during diagenesis and/or during the latest stage of post-magmatic hydrothermal alteration, as suggested by Lan (1982) and Lo (1988), and the temperature conditions in the basin were high enough to reset the argon isotopic systematics, the young plateau dates would record the time the samples cooled through the closure temperatures of dated phases, and therefore indicate the younger boundary for the age of alteration reaction. Only if the temperature condition of the basin was low and most radiogenic argon was retained in the phases, the young plateau dates can be interpreted as the possible ages for diagenetic alteration.

Implication to Cold Basins in Coastal Range

As discussed above, possible argon loss has become the most critical factor in interpreting the present $^{40}\text{Ar}/^{39}\text{Ar}$ dates for the altered glass and zeolite samples analysed in this study. Argon loss is a very common phenomenon in ^{40}Ar - ^{39}Ar dating of altered volcanic rocks or detrital K-feldspar found in basins (Walker and McDougall, 1982; Harrison and Be, 1983; Girard and Onstott, 1991). It has generally been interpreted as due to decomposition of clay minerals and volume diffusion loss from detrital phases at elevated temperatures either during a burial event and/or the irradiation procedure in the reactor because of their low decomposition temperature and relatively low argon retentivity. It is important to note that compared to natural heating events, the irradiation procedure is relatively short (10 hours), and that the temperature in the THOR Reactor during the irradiation procedure is usually lower than 45°C . Although the possibility of argon loss in the reactor can not be completely ruled out, the amount should not be substantial. Thermally-induced diffusion during burial heating may have been responsible for the argon loss before step-heating experiments.

Given the possible temperature during burial heating, the duration of heating and the grain size, the amount of argon lost from the samples can be estimated from the diffusion equation. The fraction of argon loss (F) from altered glass and zeolite during burial heating, can be estimated using the following equation given by Crank (1975) for diffusion in sphere geometry:

$$F = 1 - \frac{6}{\pi^2} \sum_{n=1}^{\infty} \frac{1}{n^2} \exp(-Dn^2\pi^2t/a^2), \text{ where } F \text{ is the fraction of argon lost; } t \text{ is the}$$

duration of heating; D, the diffusion coefficient which was calculated from D_0 (frequency factor) and E (activation energy) values by using $D = D_0 \exp(-E/RT)$, and "a" is the diffusion

size which is usually considered as the half of grain size. The diffusion parameters reported in previous studies ($D_0=8.71 \times 10^{-6} \text{ cm}^2\text{s}^{-1}$ and $A.E.=24.1 \text{ kcal mol}^{-1}$ for glass, and $D_0=1.8 \times 10^{-7} \text{ cm}^2\text{s}^{-1}$ and $A.E.=9.3 \text{ kcal mol}^{-1}$ for phillipsite) (Barrer and Vaughan, 1971; Carrol and Stolper, 1991) were adopted in the present calculations. In the calculations, a range of diffusion sizes (50-150 m) for zeolite and (1-5 m) for glass were chosen based on the crystal size observed in the samples and those suggested by Barrer and Vaughan (1971) and Carrol and Stolper (1991).

As expected, the fraction of argon lost from both glass and zeolite is positively proportional to the maximum temperature in the basin, and negatively proportional to the grain size (Fig. 4). Under a temperature condition of 65.6°C (calculated for the base of the West Taiyuan Basin at $\sim 4\text{km}$) and a geothermal gradient of 16.4°C/km (Huang *et al.*, 1993), almost all the argon would be lost from zeolite after heating for a decade and from glass after heating within 1.5 Ma (Figs. 4A and B). If the temperature condition decreases to 40°C , almost all the argon would be lost from zeolite within a few decades (Fig. 4A). Under the same temperature condition, however, the fraction of argon loss decreases to 50% for altered glass, with a diffusion size of $5 \mu\text{m}$, which might be the maximum diffusion domain size for glass (Carroll and Stolper, 1991), within 1.5 Ma (Fig. 4B). Note that the activation energies for argon diffusion in tetranatrolite, natrolite, laumontite and palagonitized glass, are not known. The employed values in the above calculations for argon loss from zeolite and glass are actually for phillipsite and fresh glass, but not for tetranatrolite, natrolite, laumontite and altered glass. It is difficult to ascertain the possible effects for such a substitution. In any case, the difference of activation energies between different species of zeolite should not be significant given their structural similarity. In addition, argon diffusion in altered phase is generally easier than that in its respective phases (see McDougall and Harrison, 1999, for a review). Thus, the above calculation results for argon loss from glass should be considered minimum values. In any case, the results of the above calculations suggest that in order to retain argon in the altered samples used in this study, the temperature conditions should not exceed 40°C . Considering the possible thickness of sedimentary sequence in the West Taiyuan Basin ($\sim 4 \text{ km}$), this temperature value would further infer an extremely low geothermal gradient ($\sim 10^\circ\text{C/km}$). This notion is generally consistent with the conclusions drawn by previous mineralogical studies ($11\sim 14^\circ\text{C/km}$) (Dorsey *et al.*, 1988, Huang *et al.*, 1993). This inferred geothermal gradient is much lower than that of foreland basins in western Taiwan ($\sim 27^\circ\text{C/km}$) (Suppe, 1984), and those found in most of orogenic basins, which are in the range of $\sim 19\sim 39^\circ\text{C/km}$ (c.f. Huang *et al.*, 1993). The rapid deposition rate in this syn-orogenic basin may have been responsible for such a low geothermal gradient.

SUMMARY

Application of the above approach in this study has led to the following conclusions:

(1) $^{40}\text{Ar}/^{39}\text{Ar}$ dating of a fresh andesite sample from the volcanic basement of the West Taiyuan Basin suggests that a volcanic eruption may have occurred at around $\sim 5.8 \text{ Ma}$, right before the arc-continent collision in Taiwan.

(2) Altered glass and zeolite samples yield similar $^{40}\text{Ar}/^{39}\text{Ar}$ dates in the range of 3.4-3.8 Ma, which is much younger than the age of the basal formation in the basin and the latest volcanism in the Coastal Range ($\sim 5 \text{ Ma}$). These plateau dates may reveal the age of diagenetic alteration if the basin remained cool enough.

(3) Retention of argon in altered glass and zeolite would further suggest that the geothermal

gradient in this orogenic basin does not exceed 10°C/km, which is much lower than those found in other ordinary basins.

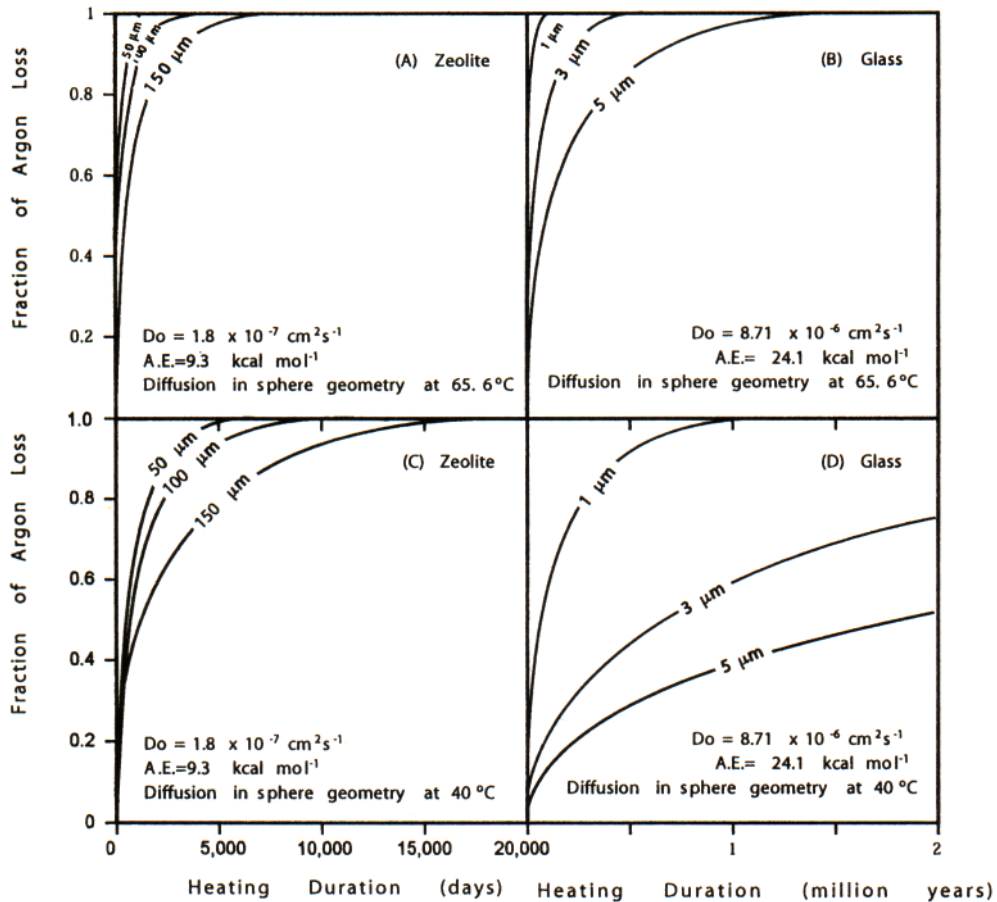


Figure 4. Calculated fraction of argon loss from zeolite (A, C) and glass (B, D), with different diffusion size (shown in the figures) during burial heating, on the basis of volume diffusion theory. Please see text for detail information about calculation method, diffusion parameters and discussion.

ACKNOWLEDGMENTS

The present communication is dedicated to Professor Chihming Wang Lee on the occasion of her seventieth birthday, and the senior author would like to sincerely thank her for her constructive advice in building up the senior author's research career. Special thanks are due to Dr. Tzen-Fu Yui for his constructive comments and review of this manuscript. This research was supported by a grant from the National Science Council (NSC89-2116-M-002-058). Thanks are also due to Miss H.F. Chen for her kind help in XRD diffraction analyses.

REFERENCES

- Barrer, R.M. and Vaughan, D.E.W. (1971) Trapping and diffusion of rare gases in philipsite, zeolite K-M and other silicates: *Trans. Faraday Soc.*, **67**, 2129-2136.
- Carroll, M.A and Stolper, E.M. (1991) Argon solubility and diffusion in silica glass: Implication for the solution behavior of molecular gases: *Geochim. Cosmochim. Acta*, **55**, 211-225.
- Chen, W.S. (1988) Tectonic evolution of sedimentary basins in Coastal Range, Taiwan: National Taiwan University Ph.D. Dissertation, 304p.
- Chi, W.R., Namson, J. and Suppe, J. (1981) Stratigraphic record of plate interactions in the Coastal Range of eastern Taiwan: *Mem. Geol. Soc. China*, **4**, 491-530.
- Crank, J. (1975) The Mathematics of Diffusion: *Clarendon Press*, Oxford, 414.
- Dorsey, R.J., Buchovecky, E.J. and Lundberg, N. (1988) Clay mineralogy of Pliocene-Pleistocene mudstones, eastern Taiwan: Combined effects of burial diagenesis and provenance unroofing: *Geology*, **16**, 944-947.
- Girard, J.P. and Onstott, T.C. (1991) Application of $^{40}\text{Ar}/^{39}\text{Ar}$ laser-probe and step-heating techniques to the dating of diagenetic K-feldspar overgrowths: *Geochim. Cosmochim. Acta*, **55**, 3777-3793.
- Gleadow, A.J.W., Duddy, I.R. and Lovering, J.F. (1983) Fission track analysis: a new tool for the evaluation of thermal histories and hydrocarbon potential: *Australian Petrol. Explor. Assoc. Jour.*, **23**, 93-102.
- Harrison, T.M. and Be, K. (1983) $^{40}\text{Ar}/^{39}\text{Ar}$ age spectrum analysis of detrital microclines from the southern San Joaquin Basin, California: an approach to determining the thermal evolution of sedimentary basins: *Earth. Planet. Sci. Lett.*, **64**, 244-256.
- Huang, C.Y., Yuan, P.B. and Teng, L.S. (1988) Paleontology of the Kangkou Limestone in the middle Coastal Range, eastern Taiwan: *Acta Geol. Taiwanica*, **26**, 133-160.
- Huang, W.L., Longo, J.M. and Pevear, D.R. (1993) An experimentally derived kinetic model for smectite-to-illite conversion and its use as a geothermometer: *Clays and Clay Minerals*, **41**, 162-177.
- Lan, C.Y. (1982) Mineralogy, petrology and hydrothermal alteration of the Chimei igneous complex, Hualien, Taiwan: *MRSO Report*, **193**, 60.
- Lanphere, M. A. and Dalrymple, G. B. (1978) The use of $^{40}\text{Ar}/^{39}\text{Ar}$ data in evaluation of disturbed K-Ar system. In: "Short Papers on the Fourth International Conference on Geochronology, Cosmochronology, Isotope Geology" (ed. R. E. Zartman): *U.S. Geol. Surv. Open File Rep.*, **78-701**, 241-243.
- Lo, C.H., Onstott, T.C., Chen, C.H. and Lee, T. (1994) An assessment of $^{40}\text{Ar}/^{39}\text{Ar}$ dating for the whole-rock volcanic samples from the Luzon Arc near Taiwan: *Chem. Geol.*, **114**, 157-178.
- Lo, C.H. and Lee, C.Y. (1994) $^{40}\text{Ar}/^{39}\text{Ar}$ Method of K-Ar Age Determination of Geological Samples Using Tsing-Hua Open-Pool (THOR) Reactor: *Jour. Geol. Soc. China*, **37**, 143-164.
- Lo, H.J. (1987) Zeolites in the Cenozoic volcanic rocks of Taiwan and the formation of zeolites in the volcanic rocks: *Mem. Geol. Soc. China*, **8**, 205-228.
- McDougall, I. and Harrison, T.M. (1999) Geochronology and Thermochronology by the $^{40}\text{Ar}/^{39}\text{Ar}$ method (2nd edit.): *Oxford University Press*, 269.
- Naeser, N.D. and McCulloh, T.H. (1989) Thermal History of Sedimentary Basins: *Springer-Verlag*, New York, 319pp.
- Odins, G.S. and 35 collaborators (1982) Interlaboratory standards for dating purposes. In: G.S. Odins (ed.) Numerical Dating in Stratigraphy, Wiley, Chichester, 123-149.

- Roddick, J.C. (1978) The application of isochron diagrams in ^{40}Ar - ^{39}Ar dating: A discussion: *Earth Planet. Sci. Lett.*, **41**, 233-244.
- Steiger, R.H. and Jager, E. (1977) Subcommittee on geochronology: Convention on the use of decay constants in geo- and cosmochemistry: *Earth Planet. Sci. Lett.*, **36**, 359-362.
- Suppe, J. (1984) Kinematics of arc-continent collision, flipping of subduction and back-arc spreading near Taiwan: *Mem. Geol. Soc. China*, **6**, 21-33.
- Suppe, J. (1988) Tectonics of arc-continent collision on both sides of the South China Sea: Taiwan and Mindoro: *Acta Geol. Taiwanica*, **26**, 1-18.
- Teng, L.S. (1990) Geotectonic evolution of late Cenozoic arc-continent collision in Taiwan: *Tectonophys.*, **183**, 57-76.
- Walker, D.A. and McDougall, I. (1982) ^{40}Ar - ^{39}Ar and K-Ar dating of altered glassy volcanic rocks: the Dabi Volcanics, P.N.G: *Geochim. Cosmochim. Acta*, **46**, 2181-2190.
- York, D. (1969) Least-squares fitting of a straight line with correlated errors: *Earth Planet. Sci. Lett.*, **5**, 320-324.

Appendix: Results of $^{40}\text{Ar}/^{39}\text{Ar}$ incremental heating experiments

T(°C)	cum. $^{39}\text{Ar}_K$	Atmos. (%)	$^{36}\text{Ar}/^{39}\text{Ar}$	$^{37}\text{Ar}/^{39}\text{Ar}$	$^{38}\text{Ar}/^{39}\text{Ar}$	$^{40}\text{Ar}/^{39}\text{Ar}$	$^{40}\text{Ar}/^{36}\text{Ar}$	Date (Ma)
DW1B altered glass								
550	.039	97.647	.95581E+00	.10091E+02	.20581E+00	.28850E+03	.30184E+03	23.7 ± 1.0
600	.052	93.711	.26712E+00	.14131E+02	.57211E-01	.83123E+02	.31118E+03	18.3 ± 1.3
650	.140	56.189	.92587E-02	.18344E-04	.10961E-01	.48979E+01	.52901E+03	7.4 ± .3
700	.496	21.908	.27809E-02	.70349E+01	.36662E-01	.13598E+01	.48900E+03	3.6 ± .1
750	.628	58.152	.66225E-02	.64633E+01	.52190E-01	.25563E+01	.38600E+03	3.7 ± .3
800	.680	79.260	.12901E-01	.34182E+00	.52703E-01	.48058E+01	.37253E+03	3.5 ± .7
850	.737	83.216	.19511E-01	.78505E+01	.28207E-01	.62461E+01	.32013E+03	3.7 ± .7
900	.768	.000	.92693E-04	.34948E+01	.13013E-01	.20679E+01	.22309E+05	7.1 ± 1.1
950	.778	86.612	.49226E-01	.15672E-03	.66844E-01	.16823E+02	.34176E+03	7.8 ± .6
1000	.817	.723	.41425E-04	.41425E-04	.90153E-02	.17214E+01	.41555E+05	5.9 ± .9
1050	.908	48.061	.60020E-02	.17702E-04	.15581E-01	.37190E+01	.61962E+03	6.7 ± .4
1100	.968	.329	.26705E-04	.26705E-04	.10875E-01	.24246E+01	.90790E+05	8.3 ± .5
1150	.991	29.764	.60755E-02	.71834E-04	.71834E-04	.60606E+01	.99754E+03	14.7 ± 6.6
1200	1.000	78.160	.37116E-01	.17576E-03	.24812E-01	.14061E+02	.37884E+03	10.7 ± 2.6

Sample mass = 500.0mg

J-value = .00193340 ± .00001197

Integrated date = 6.1 ± 0.2 Ma

Plateau date = 3.6 ± 0.1 Ma (700-850°C)

DW1W zeolite

300	.003	87.206	.57194E+00	.44449E+02	.17551E+00	.18999E+03	.33218E+03	85.2 ± 25.0
400	.007	95.314	.69618E+00	.46848E+01	.14988E+00	.21549E+03	.30954E+03	35.0 ± 19.0
500	.016	92.043	.30298E+00	.50772E-04	.68882E-01	.97299E+02	.32114E+03	26.8 ± 5.7
600	.046	91.431	.75880E-01	.10785E+02	.32438E-01	.23664E+02	.31186E+03	7.1 ± 3.5
700	.708	4.058	.71754E-03	.23132E+01	.12266E-01	.95833E+00	.13356E+04	3.1 ± .2
800	.845	36.430	.15334E-02	.16654E+01	.12501E-01	.92803E+00	.60519E+03	2.0 ± .7
900	.920	.000	.57564E-05	.19870E+01	.80423E-02	.16493E+01	.28652E+06	5.7 ± 2.2
1000	.943	33.094	.28800E-02	.18683E-04	.68226E-02	.26003E+01	.90289E+03	6.0 ± 4.0
1100	.949	95.190	.72585E-02	.71023E-04	.71023E-04	.22820E+01	.31438E+03	.4 ± 10.2
1200	1.000	49.518	.17757E-03	.77931E-01	.12096E-01	.12280E+00	.69159E+03	.2 ± 2.1

Sample mass = 400 mg

J-value = 0.00193340 ± 0 .00001197

Integrated date = 3.8 ± 0.3 Ma

Plateau date = 3.4 ± 0.3 Ma (600-1000°C)

DW2B altered glass

450	.097	90.182	.33398E+00	.46211E-04	.20102E+00	.10946E+03	.32776E+03	37.1 ± .9
510	.243	98.171	.20185E+00	.30638E-04	.14769E+00	.60786E+02	.30115E+03	3.9 ± .4
600	.275	97.837	.18730E+00	.14117E-03	.19059E+00	.56600E+02	.30219E+03	4.3 ± 1.7

680	.507	84.359	.20508E-01	.19287E-04	.23005E+00	.72123E+01	.35169E+03	3.9 ±	.3
750	.651	98.053	.11884E+00	.31118E-04	.47299E+00	.35845E+02	.30161E+03	2.4 ±	.6
870	.767	97.800	.12622E+00	.12019E+02	.59598E+00	.37239E+02	.29504E+03	2.9 ±	.7
1000	.864	90.357	.11166E+00	.13908E+02	.96861E+00	.35385E+02	.31690E+03	12.0 ±	1.2
1200	1.000	49.749	.10891E+00	.20828E+03	.40814E+00	.33170E+02	.30455E+03	66.0 ±	1.1

Sample mass = 500 mg

J-value = 0.00193340 ± 0.00001197

Integrated date = 16.2 ± 0.3 Ma

Plateau date = 3.4 ± 0.2 Ma (510 – 870°C)

DW2W zeolite

500	.187	93.231	.93576E+00	.18837E+02	.24932E+00	.29510E+03	.31536E+03	69.2 ±	1.1
600	.216	95.494	.65407E+00	.20066E-03	.30223E+00	.20242E+03	.30949E+03	31.5 ±	3.2
650	.267	98.362	.22459E+00	.53357E+02	.93748E-01	.63410E+02	.28234E+03	3.7 ±	2.5
750	.557	96.207	.82037E-01	.25678E+02	.46134E-01	.23215E+02	.28298E+03	3.1 ±	.5
850	.744	92.356	.58914E-01	.30585E+02	.40623E-01	.16383E+02	.27808E+03	4.4 ±	.6
1000	.882	86.248	.25877E-01	.43098E-04	.15848E-01	.88945E+01	.34373E+03	4.2 ±	.8
1100	.946	37.266	.11925E-01	.91433E-04	.91433E-04	.94843E+01	.79535E+03	20.6 ±	1.4
1200	1.000	42.801	.19465E-01	.14265E+02	.39658E-01	.10956E+02	.56284E+03	21.9 ±	2.8

Sample mass = 500 mg

J-value = 0.00193340 ± 0.00001197

Integrated date = 19.0 ± 0.4 Ma

Plateau date = 3.8 ± 0.4 Ma (650 - 1000°C)

DW3WR whole rock

400	.113	98.214	.74137E+00	.64513E+01	.45196E-01	.22259E+03	.30025E+03	13.9 ±	.4
500	.355	98.580	.39477E+00	.80312E+01	.19662E-01	.11775E+03	.29827E+03	5.9 ±	.3
600	.566	93.524	.88487E-01	.51645E+01	.15605E-01	.27571E+02	.31158E+03	6.2 ±	.4
650	.657	90.131	.49136E-01	.13434E+02	.17238E-01	.15015E+02	.30558E+03	5.2 ±	.7
700	.738	89.492	.48933E-01	.97012E+01	.32288E-01	.15369E+02	.31409E+03	5.6 ±	.8
760	.801	97.335	.16258E+00	.12085E+02	.41515E-01	.48451E+02	.29801E+03	4.5 ±	.6
830	.834	97.095	.19687E+00	.30182E+02	.51760E-01	.57602E+02	.29258E+03	5.9 ±	2.0
900	.860	89.293	.22932E+00	.27651E+02	.10252E+00	.73584E+02	.32088E+03	27.8 ±	2.5
1000	.933	80.531	.13174E+00	.15148E+02	.59749E-01	.46953E+02	.35640E+03	31.9 ±	.9
1100	.970	88.476	.14683E+00	.95963E+02	.46387E-01	.40892E+02	.27851E+03	17.4 ±	1.8
1200	1.000	82.830	.18568E+00	.28891E+03	.21055E-01	.39983E+02	.21533E+03	29.2 ±	2.8

Sample mass = 500 mg

J-value = 0.00193340 ± 0.00001197

Integrated date = 10.3 ± 0.2 Ma

Plateau date = 5.75 ± 0.23 (500 - 830°C)

Note:

J-value: Weighted mean of three fusions of irradiation standard LP-6 Biotite having a K-Ar age of 127.7 ± 1.4 Ma (Odin et al., 1982).

T°C = temperature with uncertainty of ± 2°C.

The date is obtained by using the following equations:

$$\text{Date} = \frac{1}{\lambda} \ln(1 + J \frac{{}^{40}\text{Ar}^*}{{}^{39}\text{Ar}_K}), \text{ and}$$

$$\frac{{}^{40}\text{Ar}^*}{{}^{39}\text{Ar}_K} = \frac{\left[\frac{{}^{40}\text{Ar}}{{}^{39}\text{Ar}} \right]_{\text{Ca}} - 295.5 \left[\frac{{}^{36}\text{Ar}}{{}^{39}\text{Ar}} \right]_{\text{m}} + 295.5 \left[\frac{{}^{36}\text{Ar}}{{}^{37}\text{Ar}} \right]_{\text{Ca}} \left[\frac{{}^{37}\text{Ar}}{{}^{39}\text{Ar}} \right]_{\text{m}}}{1 - \left[\frac{{}^{39}\text{Ar}}{{}^{37}\text{Ar}} \right]_{\text{Ca}} \left[\frac{{}^{37}\text{Ar}}{{}^{39}\text{Ar}} \right]_{\text{m}}} - \left[\frac{{}^{40}\text{Ar}}{{}^{39}\text{Ar}} \right]_{\text{K}}$$

where $[]_{\text{Ca}}$ and $[]_{\text{K}}$ = isotope ratios of argon extracted from irradiated calcium and potassium salts (values cited in the text) and $[]_{\text{m}}$ = isotope ratio of argon extracted from irradiated unknown.

Date (Ma)=the date calculated using the following decay constants: $\lambda_e = 0.581 \times 10^{-10} \text{yr}^{-1}$;

$\lambda_\beta = 4.962 \times 10^{-10} \text{yr}^{-1}$; $\lambda = 5.543 \times 10^{-10} \text{yr}^{-1}$; ${}^{40}\text{K}/\text{K} = 0.01167 \text{ atom } \%$ (Steiger and Jäger, 1977).

Cum. ${}^{39}\text{Ar}$ = cumulative fractions of ${}^{39}\text{Ar}_K$ released in each step.

The quoted error is one standard deviation and does not include the error in the interference corrections.

Integrated Date = the date and error calculated from the sum total gas from all steps; the error includes the error in J-value.

Plateau Date = the data and error calculated from the sum total gas from those steps, the ages of which fall within 2 S.D. of each other; the error includes the error in J-value.